A FINITE ELEMENT MODEL FOR PLANE STRAIN PLASTICITY WITH VELOCITY DISCONTINUITIES

H. M. VAN RIJ

The Netherlands Energy Research Foundation,
P.O. Box 1, 1755 ZG Petten, The Netherlands

SUMMARY

The proposed finite element model allows for deformation of constant strain triangular elements as well as slip between the elements. This model has three degrees of freedom at every interior node. The vertex displacements of an element depend on all three degrees of freedom. The strains within a triangular element depend on only two degrees of freedom. Moreover identical relations between strain and degrees of freedom are obtained as in the classical finite element model with a continuous displacement field. The constant slip between two elements depends only on the third degree of freedom. Hence the proposed model separates in two constituents, i.e. a classical and a slip part.

The classical part behaves just like the classical finite element model. The defining equilibrium and constitutive equations are briefly developed with the aid of the Principle of Virtual Work.

The slip part behaves like a recently developed model based on slip between rigid triangles. To obtain the necessary equilibrium and constitutive equations the edges are expanded to obtain a finite width. The Principle of Virtual Work is applied and finally the width tends to zero.Depending on the interpretation of the constitutive equations rigid perfectly plastic material properties (slip part) or elastic-perfectly plastic material properties (slip model) are obtained. The slip and classical part are interrelated along the boundaries. The reaction or action forces on both parts are identical and the boundary displacements are the sum of the displacements of both parts.

The model will be explained by means of the Prandtl punch problem. It is shown that during early loading conditions the proposed classical model behaves like the classical finite element model because velocity discontinuities are not allowed. As loading progresses a mechanism with velocity discontinuities is formed and the solution deviates from the classical results. Finally the limit load conditions are reached due to the velocity discontinuities. Hence the proposed model can be interpreted as a classical finite element model on which a slip model is superimposed which acts -due to the rigid perfectly plastic material properties- as a yield surface with built-in yielding mechanism.

The results of the proposed model are compared with those of the classical and the slip model, as well as the analytical results. It is shown that the proposed model has the advantages of both classical and slip model. However, the computational effort exceeds those of either model.

1. INTRODUCTION

The classical finite element model suffers from two potential drawbacks when applied to plane strain problems with elastic-perfectly plastic material behaviour. Due to the incompressible plastic strain increments the effectively available degrees of freedom reduce significantly, and frequently no limit load will be found [1]. Secondly perfectly plastic material may exhibit velocity discontinuities which can not be incorporated. To obtain these discontinuities a slip model [2] is developed recently, in which the triangles remain rigid. If elastic-perfectly plastic material is assumed only a relative displacement can be obtained. The proposed combined model [3] has none of the above disadvantages. Although the kinematics of the models are known for any triangular element arrangement [4, Appendix A], this paper considers only element arrangements as shown in fig. 1, for reasons of clearity.

The kinematics of the classical model are defined by horizontal and vertical dimensionless displacements u_P and v_P, defining a continuous displacement field and a piecewise constant strain field. The kinematics of the slip model are defined by dimensionless rotations θ_P, fig. 2. The rigid elements will slip relative to each other. The kinematics of the combined model allow the piecewise constant strain elements to slip relative to each other. Using the Principle of Virtual Work the static and constitutive equations are derived for the models. Section 3 discusses the boundary value problem of fig. 1. Section 4 discusses the results of this approximation of a rough Prandtl punch problem [5]. The conclusions are drawn in section 5.

2. BASIC EQUATIONS

2.1. Classical model

It is known that the vertex displacements of constant strain triangles are indistinguishable from the associated nodal displacements in the classical model. Let the nodal displacements for node P be ℓu_P, where ℓ is the length of the triangle hypotenuse of fig. 2a. The constant strains in an element are also the generalized strains. Hence for element 1 is obtained:

$$\begin{aligned} \varepsilon_x^{\,1} &= u_B - u_A \\ \varepsilon_y^{\,1} &= v_A + v_B - 2v_D \\ \gamma^1 &= u_A + u_B - 2u_D + v_B - v_A \end{aligned} \tag{1}$$

with similar relations for the other elements.

The averaged dimensionless stresses are the generalized stresses, i.e.

$$\sigma_x^{\,1} = \frac{4}{\ell^2 k} \int_A \sigma_x \,(x,y)\, dA \tag{2}$$

where k is the yield stress in shear. For any reasonably homogeneous material, constant strains will produce constant stresses, hence eq. (2) reduces to

$$(\sigma_x^{\,1},\ \sigma_y^{\,1},\ \tau^1) = (1/k)\ (\sigma_x,\ \sigma_y,\ \tau) \tag{3}$$

The virtual internal work due to a virtual displacement ℓu_D (fig. 2a) becomes for element 1:

$$W_{int} = \int_{ABD} (\sigma_x \varepsilon_x + \sigma_y \varepsilon_y + \tau\gamma)\, dA = -\, k\, \tau^1\, \ell^2 u_D \,/\, 2 \tag{4}$$

The total virtual work due to ℓu_D becomes

$$W_{int} = (k\,\ell^2/2)\; u_D\; (-\tau^1 - \sigma_x^{\,2} + \tau^3 + \sigma_x^{\,4}) \tag{5}$$

In absence of forces at node D the virtual external work is zero, hence the horizontal and vertical equilibrium equation for a generic small node are

$$\sigma_x^{\,2} - \sigma_x^{\,4} + \tau^1 + \tau^3 = 0 \tag{6a}$$

$$\sigma_y^{\,1} - \sigma_y^{\,3} + \tau^2 - \tau^4 = 0 \tag{6b}$$

Similarly the equations for a generic large node are (fig. 2b):

$$\sigma_x^{\,1} + \sigma_x^{\,2} + \sigma_x^{\,3} + \sigma_x^{\,4} - \sigma_x^{\,5} - \sigma_x^{\,6} - \sigma_x^{\,7} - \sigma_x^{\,8} + \tau^1 + \tau^2 - \tau^3 - \tau^4 - \tau^5 - \tau^6 + \tau^7 + \tau^8 = 0 \tag{6c}$$

$$\sigma_y^{\,1} + \sigma_y^{\,2} - \sigma_y^{\,3} - \sigma_y^{\,4} - \sigma_y^{\,5} - \sigma_y^{\,6} + \sigma_y^{\,7} + \sigma_y^{\,8} + \tau^1 + \tau^2 + \tau^3 + \tau^4 - \tau^5 - \tau^6 - \tau^7 - \tau^8 = 0 \tag{6d}$$

Elastic-perfectly plastic material under plane strain conditions is assumed. The constitutive equations, used for a generic element α, are:

$$\begin{aligned}
&f^\alpha = (\sigma_x^{\,\alpha} - \sigma_y^{\,\alpha})^2/4 + (\tau^\alpha)^2 \le 1 \qquad \dot\lambda^\alpha \ge 0 \\
&\dot\sigma_x^{\,\alpha} = 2\,(G/k)\,[\dot\varepsilon_x^{\,\alpha} + \nu\,(\dot\varepsilon_x^{\,\alpha} + \dot\varepsilon_y^{\,\alpha})/(1-2\nu)] - \dot\lambda^\alpha\,(\sigma_x^{\,\alpha} - \sigma_y^{\,\alpha})/2 \\
&\dot\sigma_y^{\,\alpha} = 2\,(G/k)\,[\dot\varepsilon_y^{\,\alpha} + \nu\,(\dot\varepsilon_x^{\,\alpha} + \dot\varepsilon_y^{\,\alpha})/(1-2\nu)] - \dot\lambda^\alpha\,(\sigma_y^{\,\alpha} - \sigma_x^{\,\alpha})/2 \\
&\dot\tau^\alpha = (G/k)\,\dot\gamma^\alpha - \dot\lambda^\alpha\tau^\alpha \\
&\text{IF } f^\alpha < 1 \text{ OR } \dot f^\alpha < 0 \text{ THEN } \dot\lambda^\alpha = 0 \text{ ELSE } \dot\lambda^\alpha = (G/2k)[(\sigma_x^{\,\alpha} - \sigma_y^{\,\alpha})(\dot\varepsilon_x^{\,\alpha} - \dot\varepsilon_y^{\,\alpha}) + 2\tau^\alpha\dot\gamma^\alpha]
\end{aligned} \tag{7}$$

where G is the shear modulus and ν is Poisson's ratio.

2.2. Slip model

The elementary slip mechanisms are shown in fig. 2. It is observed [4] that the slip across the two edges of a diagonal are equal, hence each diagonal, horizontal, and vertical edge has only one slip. A dimensionless generalized strain ω is defined for a generic edge PQ by

$$\omega_{PQ} = d_{PQ}\;\ell_{PQ}\;/\;\ell^2 \tag{8}$$

where d_{PQ} is the slip across and ℓ_{PQ} the length of edge PQ. The only non-zero strains due to the mechanisms of fig. 2 are:

$$\theta_D \equiv \omega_{FG} = \omega_{GB} = \omega_{BA} = \omega_{AF} = -\tfrac{1}{2}\,\omega_{AG} = -\tfrac{1}{2}\,\omega_{BF} \tag{9a}$$

$$\theta_G \equiv \omega_{FL} = \omega_{LH} = \omega_{HB} = \omega_{BF} = -\omega_{FG} = -\omega_{LG} = -\omega_{HG} = -\omega_{BG} \tag{9b}$$

The total strain in an edge is the resultant of several mechanisms. For edge BF and FG these strains are:

$$\omega_{BF} = \theta_A + \theta_G - 2\theta_D \qquad \text{and} \qquad \omega_{FG} = \theta_D + \theta_I - \theta_F - \theta_G \tag{10a,b}$$

with similar relations for the other edges.

The generalized strain in an edge can be related to the continuum strains by expanding an edge to a small rectangular domain with a small thickness $\ell\delta$.

The non-zero strain in a generic edge PQ becomes:

$$\gamma_{xy} = d_{PQ} \,/\, (\ell\delta) = \omega_{PQ}\, \ell/(\ell_{PQ}\delta) \tag{11}$$

The associated generalized stress of edge PQ, defined similarly as eqs. (2) and (3), is

$$\tau_{PQ} = \lim_{\delta\to 0} \int_A \frac{\tau_{xy}\, dA}{k\, \ell_{PQ}\, \ell\delta} = \frac{\tau_{xy}}{k} \tag{12}$$

The virtual internal work done in edge PQ is:

$$W_{int} = k\ell^2\, \tau_{PQ}\, \omega_{PQ} \tag{13}$$

If no virtual external work is done with the mechanisms of fig. 2 the equilibrium equations, using eq. (9), become

$$\tau_{FG} + \tau_{GB} + \tau_{BA} + \tau_{AF} - 2\tau_{AG} - 2\tau_{BF} = 0 \tag{14a}$$

$$\tau_{FL} + \tau_{LH} + \tau_{HB} + \tau_{BF} - \tau_{FG} - \tau_{LG} - \tau_{HG} - \tau_{BG} = 0 \tag{14b}$$

In analogy with eq. (7) the constitutive behaviour for edge PQ becomes, using eqs. (11) and (12):

$$\tau_{PQ}^2 \le 1 \tag{15a}$$

$$\text{IF } \tau_{PQ}^2 < 1 \text{ OR } \lim_{\delta\to 0} (\tau_{PQ}\, \dot{\omega}_{PQ}/\delta) < 0 \tag{15b}$$

$$\text{THEN } \dot{\tau}_{PQ} = \lim_{\delta\to 0} (G\ell/k\, \ell_{PQ}\, \delta)\, \dot{\omega}_{PQ} \qquad \text{ELSE } \dot{\tau}_{PQ} = 0 \tag{15c,d}$$

The latter eq. (15b) corresponds with the $\dot{\lambda}^{\alpha}$ from eq. (7). The elastic branch of eq. (15c) can not be used as stated when the limit is taken. In the slip model this dilemma is solved by defining a finite "slipmodulus" G/δ, and multiplying the latter equation (15b) with δ. Hence the slip model behaves like an elastic-perfectly plastic material. The obtained displacement field depends on this unknown "slipmodulus". For a known G the "slipmodulus" can not be used. This dilemma is solved by assuming the edges to behave as rigid perfectly plastic material. The kinematic variables are then defined as:

$$\begin{aligned} \omega_{PQ} &= \omega_{PQ}^0 + \omega_{PQ}^1\, \delta \\ \theta_P &= \theta_P^0 + \theta_P^1\, \delta \end{aligned} \tag{16}$$

If the elastic branch is used, eq. (15c), then $\dot{\omega}_{PQ}^0$ vanishes and the limit of the latter eq. (15b) remains finite. If the plastic branch is used, eq. (15d), then $\dot{\omega}_{PQ}^0$ may be non-zero, in which case the limit of the latter eq. (15b) becomes either positive or negative infinite, but inequality can still be verified. In view of eq. (16) this implies that an elastic edge with an effectively zero strain rate still allows for a non-zero stress rate when δ tends to zero. The rigid perfectly plastic constitutive behaviour for the slip model becomes:

$$\tau_{PQ}^2 \le 1 \tag{17a}$$

$$\text{IF } \tau_{PQ}^2 < 1 \text{ OR } \lim_{\delta\to 0} \{\tau_{PQ}\, (\dot{\omega}_{PQ}^1 + \dot{\omega}_{PQ}^0/\delta) < 0 \tag{17b}$$

$$\text{THEN } \dot{\omega}_{PQ}{}^{0} = 0 \text{ AND } \dot{\tau}_{PQ} = (G\ell/k\ \ell_{PQ})\ \dot{\omega}_{PQ}{}^{1} \quad \text{ELSE } \dot{\tau}_{PQ} = 0 \tag{17c,d}$$

2.3. Combined model

In the combined model u_P, v_P and θ_P are the three generalized displacement variables. The four drawn vertex displacements in fig. 2b become:

$$\bar{u}_1 = \ell\, u_F + \ell(2\theta_D - \theta_F - \theta_G)/2 \tag{18a}$$

$$\bar{u}_2 = \ell(u_F + v_F)/\sqrt{2} - \ell(\theta_G - \theta_D)/2 \tag{18b}$$

$$\bar{u}_3 = -\ell u_G - \ell(2\theta_D - \theta_F - \theta_G)/2 \tag{18c}$$

$$\bar{u}_4 = \ell\, u_F - \ell(2\theta_I - \theta_F - \theta_G)/2 \tag{18d}$$

with similar equations for other vertex displacements.

This eq. demonstrates that the generalized displacements u_F and v_F do not have a physical meaning, but are convenient variables. The cartesian displacements in vertex F of element 7 can be obtained by a transformation of eqs. (18a) and (18b). Also can be verified that the displacement component normal to an edge is continuous. The slip across edge FG becomes

$$d_{FG} = \bar{u}_1 - \bar{u}_4 = \ell(\theta_D + \theta_I - \theta_F - \theta_G) \tag{19}$$

The elongation of edge FG of triangle 7 becomes

$$\varepsilon_x{}^{7} = -(\bar{u}_1 + \bar{u}_3)/\ell = u_G - u_F \tag{20}$$

with similar relations for the remaining strains. Eq. (20) is similar to eq. (1) from the classical model. The slip strain, using eqs. (8) and (19), is stated in eq. (10b). Hence it is shown that the combined model separates into a classical and a slip part. Therefore the corresponding strain-displacement, constitutive and equilibrium equations can be used as derived in the two preceding subsections.

3. BOUNDARY VALUE PROBLEM

The number of equations and unknowns must be equal. For every generalized strain and stress unknown there is a strain-displacement relation and a constitutive relation respectively. Hence every displacement unknown must be balanced by an equilibrium equation. The non-prescribed displacements along the boundary have similar equilibrium equations as derived in the preceding section.

3.1. Classical model

Along the boundaries F-M and M-S of fig. 1 u_P and v_P are zero respectively. Furthermore

$$v_F = v_G = -v_o \tag{21a}$$

$$u_S = u_T = u_U = u_V = u_W = u_X = u_A = u_o \tag{21b}$$

The associated equilibrium equations of the displacements of eq. (21) are

$$T_2 = \frac{1}{6\ell k}\int_0^{6\ell} T_n\,(y)\,dy = \frac{1}{24}\sum_{i=1}^{6}\left\{-(\sigma_x^{i1} + \sigma_x^{i3} + 2\sigma_x^{i4}) + (\tau^{i1} - \tau^{i3})\right\} \tag{22a}$$

$$T_1 = \frac{1}{\ell k} \int_0^{\ell} T_n(x)dx = \frac{1}{4}(-\sigma_y^{71} - \sigma_y^{72} - 2\sigma_y^{81} - \sigma_y^{82} - \sigma_y^{84} - \tau^{71} - \tau^{72} - \tau^{82} + \tau^{84}) \qquad (22b)$$

Eq. (22) serves to compute the reaction forces if u_o and v_o are prescribed.

3.2. Slip model

If all θ_P are taken equal in fig. 1 the entire domain remains unchanged as appears from eq. (10). Hence θ_M can arbitrarily be set equal to zero. The boundary displacements are incorporated by placing fictitious elements along the outside of the domain. These elements can move as a mechanism tangent to the boundary. In absence of traction forces and prescribed displacements in this direction, this results in zero strains in the boundary edges. To satisfy the suppressed boundary conditions all θ_P are set zero along G-M and M-S boundary. The remaining boundary conditions are given by

$$\theta_A/12 = \theta_X/10 = \theta_W/8 = \theta_V/6 = \theta_U/4 = \theta_T/2 = u_o \qquad (23a)$$

$$\theta_F/2 = -v_o \qquad (23b)$$

The associated equilibrium equations are

$$T_1 = -2(\tau_{EF'} - \tau_{FF'} + \tau_{GF'}) + \tau_{FG} \qquad (24a)$$

$$T_2 = \frac{1}{3}[(\tau_{ST'} - \tau_{TT'} + \tau_{UT'}) + 2(\tau_{TU'} - \tau_{UU'} + \tau_{VU'}) + 3(\tau_{UV'} - \tau_{VV'} + \tau_{WV'}) + 4(\tau_{VW'} - \tau_{WW'} + \tau_{XW'}) + 5(\tau_{wx'} - \tau_{XX'} + \tau_{AX'}) + 6\tau_{XB}] \qquad (24b)$$

The last term in eq. (24a) is due to the zero tangential motion along F-G.

3.3. Combined model

The combined model is the superposition of the classical and slip model. For either part of the combined model rigid body motions must be suppressed. In view of the boundary conditions in fig. 1 this implies that the suppressed displacements in the preceding two subsections remain suppressed. Replacing u_o and v_o in eq. (21) by u_{oc} and v_{oc}, and in eq. (23) by u_{os} and v_{os}, each of the slip displacements subdivided as demonstrated in eq. (16), the total boundary displacements along S-XA and F-G become

$$u_o = u_{oc} + u_{os}^0 + u_{os}^1 \delta \qquad (25a)$$

$$v_o = v_{oc} + v_{os}^0 + v_{os}^1 \delta \qquad (25b)$$

The forces T_1 and T_2 are identical in either part.

The solution technique is explained with the boundary value of fig. 1 with u_o suppressed and v_o slowly increased. If v_o is sufficiently small all classical and slip elements follow the elastic branch of their constitutive behaviour, i.e. eqs. (7) and (17). Hence u_{os}^0 and v_{os}^0 are zero and for δ tends to zero this implies $u_{oc} = 0$ and $v_{oc} = v_o$.

The classical model can now be solved. Eq. (22) is used to compute T_1 and T_2, which are then used in eq. (24) to solve the slip model. The combined model solution consists out of a series of sequential solution of the classical and slip model, causing classical and slip elements to yield. Increasing loading conditions will cause the yielded slip elements to form a mechanism allowing for a non-zero $\dot{u}_{os}^0$ and $\dot{v}_{os}^0$.

The motion likely to occur is that a velocity downwards along FG pushes boundary S-XA to the left, which implies for the classical model that

$$\dot{u}^0_{oc} = -\dot{u}^0_{os} = \dot{v}^0_{os}/6 \text{ and } \dot{v}^0_{oc} = \dot{v}^0_o - \dot{v}^0_{os} \tag{26}$$

The motion associated with $\dot{v}_{os}$ does not involve any additional external work. Hence

$$6\dot{T}_2\dot{u}^0_{os} + \dot{T}_1\dot{v}^0_{os} = 0 \qquad \text{OR} \qquad \dot{T}_1 = \dot{T}_2 \tag{27}$$

which supplies an additional equation for $\dot{v}^0_{os}$.

To suppress the yielding mechanism of the slip model $\dot{u}^1_{os}$ is set equal to zero and $\dot{T}_1$ is the interaction force between the classical and slip model. The solution of the combined model is again obtained by the sequential solution of the classical and slip model. As v_o increases more elements will yield. Eventually a second slip mechanism will be formed, i.e. $\dot{u}^0_{os}$ and $\dot{v}^0_{os}$ become independent. Neither mechanism will cause an increase in the external work rate, hence $\dot{T}_1 = \dot{T}_2 = 0$ and limit load conditions are reached.

4. EXAMPLE

The rough Prandtl punch problem [5] was simulated by placing an elastic-perfectly plastic material (Poisson's ratio .3) under plane strain conditions in a smooth box, which is idented with a rigid punch (fig. 1). The yielding sequence of the elements in the combined model is shown in fig. 3. The classical and slip model yielding sequences are given in [3,4]. The load deflection curve for all models is shown in fig. 4. The combined model solution occurs as described in the previous section. Even though continuous loading conditions were prescribed, a significant unloading occurred in the classical elements at the beginning of stage 77. The linearization of $\dot{f}^\alpha$ in eq. (7) causes an increase in f. The stiffness matrix is recomputed when f^α increased .001 in one stage without yielding of any classical element. This occurred at the end of stages 19, 25, 29, 34, 38, 45, 51, 55, 57, 68, 77 through 80, 84, 87 and 89. The slip model was complicated by undetermined displacement unknowns. If for example all edges of fig. 2a are at yield the associated equilibrium equation turns into an identity. The latter eq. (17b) can be used to find the range of the displacement. Details are given in [4]. Stage 115 of the classical model is 14% above the combined model yield point load. At stage 153 when more than half the number of elements have yielded this yield load is exceeded by 30%. Due to a numerical instability no limit load could be found with the classical model.

5. CONCLUSIONS

In the fully elastic range the results of the classical and combined model, both being compressible, are in good agreement with the analytical results of the semi-infinite domain obtained by Green and Zerna [6]. The same holds for the incompressible slip model. The plastic regions develop in a reasonable fashion. The limit load of the classical model amounts to 7.23 and is obtained by applying the limit load theorems to the element arrangement of fig. 1 [4]. The limit load of 6.0, obtained with the slip as well as combined model, is a reasonable upperbound of the analytical value of 5.14. The computations were carried out on a CDC-Cyber 74. The CPU sec per degree of freedom were for the slip, classical and combined model, .44, .55 and .62 respectively. More efficient programming will reduce these times, but their relative magnitudes are probably meaningful. The combined model shows a superior elastic-plastic behaviour compared to either the classical and slip model.

6. ACKNOWLEDGEMENTS

This research was sponsored by the Office of Naval Research and partially sponsored by the University of Minnesota Computer Center. The results are taken from the authors dissertation [4] submitted to the University of Minnesota. The author wishes to thank his advisor, Prof. P.G. Hodge Jr., for his guidance.

7. REFERENCES

[1] NAGTEGAAL, J.C., PARKS, D.M., RICE, J.R., "On numerical accurate finite element solutions in the fully plastic range", Comp. Meth. Appl. Mech. & Engr. 4, 153-177 (1974).

[2] VAN RIJ, H.M., HODGE, Jr., P.G., "A slip model for finite element plasticity", J. Appl. Mech. 45, 527-532 (1978).

[3] HODGE, Jr. P.G., VAN RIJ, H.M., "A finite element model for plane-strain plasticity", AEM-report H1-22, University of Minnesota (1978).

[4] VAN RIJ, H.M., "Finite element model with velocity discontinuities", Ph.D. Dissertation, University of Minnesota (1978).

[5] PRANDTL, L., "Ueber die Härte plastischer Körper", Göttinger Nachr., Math. Phys. KL 1920, 74-85 (1920).

[6] GREEN, A.E., ZERNA, W., "Theoretical elasticity", Oxford Clarendon Press (1954).

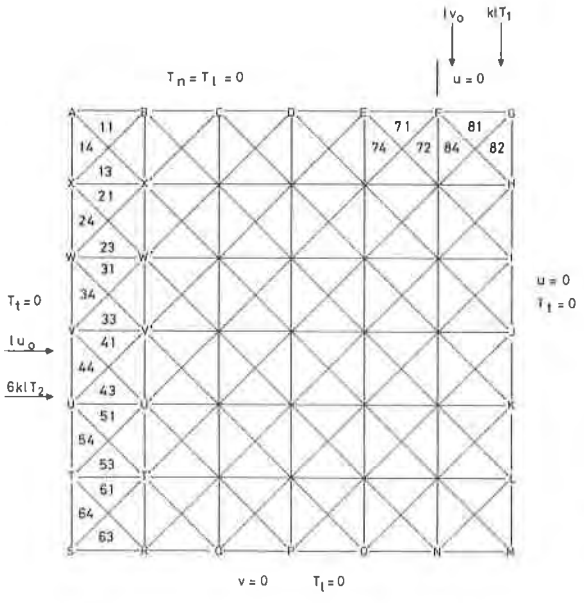

Fig. 1 Element arrangement.

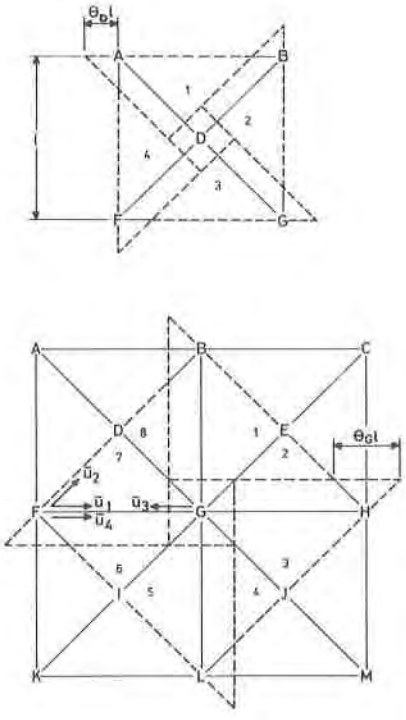

Fig. 2 Small (a) and large (b) node mechanism.

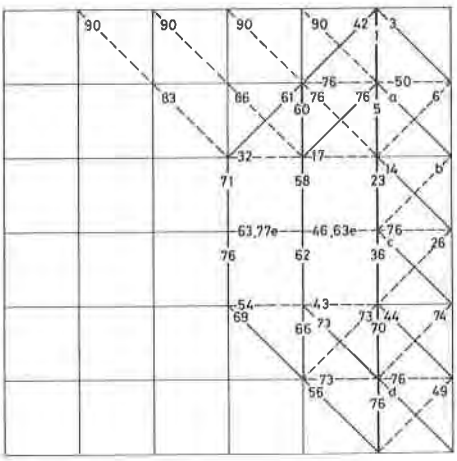

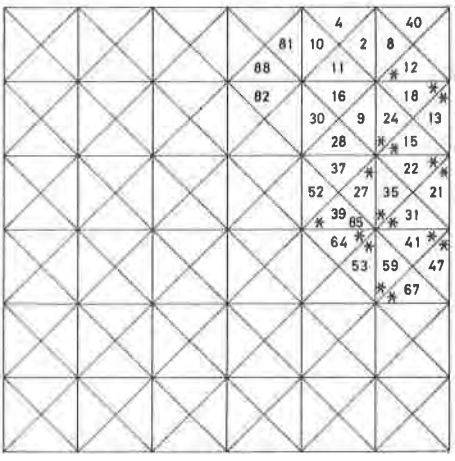

Fig. 3 Yielding sequence in edges (a) and triangles (b).

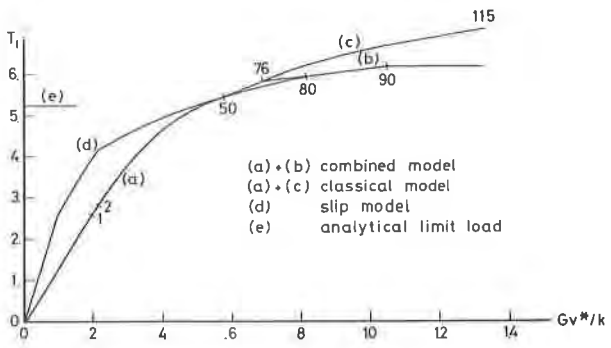

Fig. 4 Load deflection curves.